Postprint of: Tylingo R., Kempa P., Banach-Kopeć A., Mania S., A novel method of creating thermoplastic chitosan blends to produce cell scaffolds by FDM additive manufacturing, CARBOHYDRATE POLYMERS, Vol. 280 (2022), 119028, DOI: 10.1016/j.carbpol.2021.119028

Article

A novel method of creating thermoplastic chitosan blends to produce cell scaffolds by FDM additive manufacturing

Robert Tylingo[1#], Piotr Kempa[2], Adrianna Banach-Kopeć[1], Szymon Mania[1#*]

[1] Chemical Faculty, Department of Chemistry, Technology and Biotechnology of Food, Gdansk University of Technology, 11/12 G. Narutowicza Str., 80-233 Gdansk, Poland; robertt@pg.edu.pl (R.T.), adrianna.banach@pg.edu.pl (A.B-K.), szymon.mania@pg.edu.pl (S.M.)

[2] Chitone Sp. z o. o. 15 Pionierów Str., 84-300 Lębork, Poland; p.kempa@chitone.pl (P.K.)

***Correspondence:** szymon.mania@pg.edu.pl, Tel.: +48-58-347-28-56

Abstract:

Due to its remarkable and promising biological and structural properties, chitosan has been widely studied in several potential applications in the biomedical sector. Attempts are being made to use this polymer and its properties in thermoplastics dedicated to 3D printing in FDM technology. However, chitosan can be processed only from acid solution, which limits its applications.The paper presents a new path for the production of filaments based on unstable chitosan hydrogels obtained by carbon dioxide saturation, as well as synthetic polymers such as polyvinyl alcohol and polycaprolactone. The results confirm that the absence of acid allows formation of thermally stable and printable filaments containing from 5% to 15% of chitosan, capable of reducing *S. aureus* and *E. coli* bacteria by 0.41-1.43 in logarithmic scale (56 – 94%) and 0.28-0.94 in logartithimc scale (36 – 89%), respectively.

Keywords: 3D printing; chitosan; polycaprolactone; filament; antimicrobial properties

1. Introduction

Creating polymer compositions by physical mixing or chemical coupling is one of the most popular ways of producing materials with novel properties. These properties may correlate with the concentration of components present in the created composites or give them completely new and non-obvious features (Rajeswari, Sreerag Gopi, Jackina Stobel Christy Jayaraj, & Pius, 2020). Polymers from renewable sources deserve particular attention because of their low cost, high availability, non-toxicity and ability to be used in products from sustainable resources. Chitosan (CS) is an example of such a resource. Chitosan is the product of chitin deacethylation, composed of randomly distributed ß(1→4)-linked D-glucosamine and N-acetyl-D-glucosamine units in a linear polymer structure. The sources of chitin are exoskeletons of shellfish and insects, as well as the cell walls of fungi (Muzzarelli, 2009). Due to its biocompatibility, biodegradability, antimicrobial properties, non-toxicity, and film-forming properties, chitosan offers potential in a range of applications (Rinaudo, 2006).The major challenge in the efficient production of renewable polymers is the compatibility of the raw material with common industrial processing methods such as extrusion, injection moulding and extrusion blow moulding. Over the last few years, the meltability of thermoplastic polymers has been strongly focused on the versatility of production by 3D printing

# These authors contributed equally to this paper.

methods with a particular focus on the fused deposition method (FDM), which is based on creating three-dimensional products by melting the raw material and depositing it on previously produced layers of solidified material (Mania, Banach, & Tylingo, 2020). Despite a number of advantages, the use of chitosan in the above methods is very limited as it does not melt. Therefore, obtaining composites with biological properties resulting from the characteristics of intempersible biopolymers, such as antimicrobial activity, is still very restricted.

In the scientific literature, there are examples of studies that attempted to overcome this limitation. The simplest methods are the use of additives of chitosan or other biopolymers as a solid material in the form of particles in the polymer matrix, which guarantees the meltability of the material (Bonilla, Fortunati, Vargas, Chiralt, & Kenny 2013; Correlo et al., 2009). This solution is effective when chitosan, as a filler, is used in concentrations of 0.5 - 1.5% (Rojas-Martínez et al., 2020). Our previous work has shown that direct co-extrusion of chitosan with a poly(lactic acid) (PLA) matrix hinders the achievement of homogeneous and smooth 3D printing filaments. The filaments containing more than 3% of chitosan in PLA matrix were not suitable for FDM printing and had weak antimicrobial properties (Mania et al., 2019).

Epure et al. have modified the physicochemical properties of chitosan to make it thermoplastic. Chitosan in powder form was mixed with glycerol and 2% acetic acid was added to form a plastic paste which was pressed hot. The addition of glycerol made the product extendable and therefore it did not crumble (Epure, Griffon, Pollet, & Avérous, 2011). However, it was not possible to completely melt the chitosan and the final colour of the mixture was darkened in the presence of acetic acid.

Grande, Pessan and Carvalho (2015) proposed a method of obtaining a plastic chitosan composite with PLA. It consisted of mixing 1% chitosan solution in acetic acid with 1% poly(vinyl alcohol) (PVA) solution as a compatibility enhancer and using glycerol as a plasticizer (Grande, Pessam, & Carvalho, 2015). The mixture was gently dried, ground and re-dried and then mixed with PLA granules. The method developed made it possible to obtain thermoplastic filaments but did not solve the problem of polymer degradation, which results from the residual acid used to dissolve the chitosan. The authors indicated severe degradation of chitosan and of PLA leading to a decrease in the mechanical properties and strong darkening during processing, even when the PVA-chitosan blend was dried at mild temperatures (<50°C). Thus, the extraction of acid residues proved to be an obstacle to overcome.

Other research groups have also worked on obtaining thermoplastic chitosan using polyols, water and acetic acid as an alternative to the thermomechanical method (Dang & Yoksan, 2015; Mendes et al., 2016). Although this approach reduced the size of the dispersed chitosan phase to a few microns, the irregular geometry of the dispersed phase indicated that chitosan was not effectively melted during thermo-mechanical mixing. Unfortunately, the problem of the darkening of the resulting mixtures has still not been solved and has intensified with the increase in chitosan concentration in composites (Matet, Heuzey, Pollet, Ajji, & Avérous, 2013).

Grande, Pessan and Carvalho (2018) suggested a way to obtain thermoplastic PLA, PVA and chitosan blends. The first stage consisted of mixing a 1% solution of PVA and a 1% solution of chitosan in 1% acetic acid, which was then spray-dried, while the volatile acetic acid at the drying

temperature was driven away together with water. Another way was to freeze the mixture of solutions and subject it to freeze-drying. However, it must be taken into account that the evaporation of acetic acid from the material during sublimation may not always be efficient and may result in increased exploitation of the apparatus on an industrial scale (Grande, Pessan, & Carvalho, 2018). Target composites presented by the authors contain from 2.5 to 6.25% chitosan and the studies do not present the effect of long-term processing of the composite at extrusion temperature.

In in our work, we tried to confirm the hypothesis that the elimination of acid during chitosan dissolution will allow obtaining thermoplastic and thermostable filaments in a PCL matrix with antimicrobial activity. This effect was attempted by using an innovative method of saturation with gaseous carbon dioxide for the processing of chitosan in the form of a solution. To date, such an approach to obtain thermoplastic chitosan composites has not been proposed in the scientific literature.

2. Experimental methods

2.1. Materials

Medium molecular weight chitosan (MMW) with deacetylation degree of 81-96% was purchased from Primex (Iceland). PVA with molecular weight of 9-10 kDa and a degree of hydrolysis of 80% was purchased from Merck (Germany). Medium molecular weight PCL with a melting index equal to 11 g/10 min at 100°C was purchased from Esun Industrial Co., Ltd. (Shenzhen, China). The acetic acid, hydrochloric acid and sodium hydroxide were produced by Avantor Performance Materials Poland S.A (Gliwice, Poland). The carbon dioxide used to saturate the chitosan preceipitate was derived from Linde Gaz Polska Sp. z o. o. (Gdańsk, Poland). For microbiological tests, the following bacterial strains were used: Gram (−) *Escherichia coli* (ATCC 25922) and Gram (+) *Staphylococcus aureus* (ATCC 29213) from the Polish Collection of Microorganisms, Ludwik Hirszfeld Institute of Immunology and Experimental Therapy of the Polish Academy of Sciences (Wrocław, Poland). Phosphate Buffered Saline (PBS), Tryptic Soy Agar (TSA), and Tryptic Soy Broth (TSB) media were purchased from Merck (Germany).

2.2. Preparation of CS/PVA composites

Chitosan/poly(vinyl alcohol) (CS/PVA) composites were made in three variants: 1% CS solution in 0.1M acetic acid, 1% CS solution in 0.1M hydrochloric acid, and 1% CS solution in carbonic acid.

The 1% CS solution in 0.1M acetic acid and 0.1M hydrochloric acid was obtained by indirect dissolving of polymer in acid solution under mechanical stirring at a speed of 300 RPM (RA 2020, Heidolph Instruments GmbH & Co. KG, Kelheim, Germany) until a homogenous and clear solution was obtained (3 hours). The 1% chitosan solution in carbonic acid (CS-CO_2) was prepared according to the methodology proposed by Gorczyca and colleagues with slight modifications (Gorczyca et al., 2014).

In the first step, 1.5% CS solution in 0.1M acetic acid was obtained by indirect dissolution of polymer in proper acid solution during mechanical stirring at a speed of 300 RPM (RA 2020, Heidolph Instruments GmbH & Co. KG, Kelheim, Germany). Then, during mixing, 0.5M solution of sodium hydroxide was added until a pH value in the range of 9-10 was reached. This was equivalent to complete precipitation of chitosan in the microcrystalline form. The precipitated

chitosan was filtered with the use of a seepage kit under reduced pressure and was washed several times with distilled water until the pH of the rinsing water reached a value equal to 7.0. Finally, the precipitated chitosan was weighed and suspended in such an amount of distilled water to obtain a solution of 1 % in relation to the dry matter of the polymer. The CS suspension was homogenized at 10000 RPM for 3 minutes (Silent Crusher M, Heidolph Instruments GmbH & Co. KG, Kelheim, Germany) and then saturated with CO_2 with simultaneous mechanical mixing using a hollow shaft stirrer for gas saturation (BIOMIXBMX-10, Gdańsk, Poland) until completely dissolved.

The PVA solution was made by heating distilled water to 60°C and adding to it small portions of the appropriate amount of PVA to obtain a concentration of 1%. The mixture was strongly mixed with simultaneous heating to 50-60°C (MR Hei-Standard, Heidolph Instruments GmbH & Co. KG, Kelheim, Germany). After obtaining a homogeneous solution, it was cooled to room temperature. The finished PVA solution and chitosan solution dissolved in hydrochloric or acetic or carbonic acid were mixed at a 1:1 mass ratio, frozen at -24°C and then freeze-dried for 72 h (p = 0.94 mbar, sample temperature 20°C, condenser temperature -80°C; Christ Alpha 12–4 LD Plus, Osterode am Harz, Germany).

2.3. Evaluation of the effect of extrusion time on the colour of CS/PVA composite

Freeze-dried PVA/chitosan composites were ground in a laboratory mill (ChemLand, FW 135, Stargard, Poland) to obtain fine chips (approx. 5 s). The crushed material was placed in glass petri dishes with lids, which were then placed in a laboratory oven heated to 150°C (BINDER FDL 115, Gmbh, Tuttlingen, Germany). The process of heating the composites was carried out for 4 hours. The results were presented in the form of photos of the composites taken before heating and after 1, 2, 3 and 4 hours of heating (Nikon D7200 camera (Kumagaya, Japan).

2.4. Filament preparation

To produce thermoplastic filaments based on chitosan, poly(vinyl alcohol) and polycaprolactone, in the first stage CS-CO_2/PVA composites were prepared by mixing 1% CS-CO_2 solution and 1% PVA solution in 3:1, 1:1, 1:3 mass ratios and freeze-drying for 72 hours (p = 0.94 mbar, sample temperature 20°C, condenser temperature -80°C; Christ Alpha 12–4 LD Plus, Osterode am Harz, Germany). The dry CS-CO_2/PVA composites were ground in a laboratory mill (ChemLand, FW 135, Stargard, Poland), until a fine powder was obtained. Prior to the extrusion process, an extruder was started (Wellzoom C, Zhenzen, China), setting a temperature of 150°C in the dosing and extrusion zone. When the temperature was reached, the milled material was placed in the dispenser of the extruder and the dosing auger drive was started. The extrusion process was carried out at a speed of 2000 mm/min. The molding nozzle diameter was equal to 1.75 mm. The resulting extrudate was cut by hand into sections not exceeding 3 mm in length. The CS-CO_2/PVA/PCL filaments were produced by mixing 80g of PCL granules and 20g of selected CS-CO_2/PVA composite granules and extrusion. The thoroughly mixed combination was then re-extruded using the same extruder and the same extrusion conditions as were used to produce granules of the CS-CO_2/PVA composites.

2.5. 3D Print Preparation

The CAD model in the form of a 12.5 mm diameter and 20 mm high cylinder was created with AutoCAD 2019 software and exported in "stl" format. The file was converted to "gcode" using Z-

Suite V 2.12.0.0 software. The object was printed using the FDM technique with a Zortrax M200 Plus printer (Olsztyn, Poland) with working space dimensions 200 x 200 x 300 mm. Printing parameters for control (PCL) and CS-CO_2/PVA/PCL filaments were as follows: extruder nozzle size 0.4mm, layer height 0.1mm, print filling: 30%, print temperature: 150°C, working field temperature: 30°C.

2.6 Material characterization

2.6.1 Morphological evaluation (SEM)

The topography of the filaments was evaluated using a VP-SEM S3400-N scanning electron microscope (Hitachi, Hyogo, Japan). The acceleration voltage was 25 kV. Compensation of the charge was ensured by recording the images at a vacuum of 120 Pa and using a back-scattering electron detector (BSE). The use of the BSE detector allowed increase of the contrast of local areas differing in mass and/or density of the material. Visual recording of the samples was obtained with Nikon D7200 (Warsaw, Poland).

2.6.2. Chemical structure (FTIR)

FT-IR spectra have been recorded using a spectrometer (Nicolet 8700; Thermo Electron Corp., Waltham, MA, USA) equipped with GoldenGate (Specac Corp., Oprington, UK) with a single-reflection diamond. The temperature of the crystal was maintained at 25.0 ± 0.1°C during measurement. 64 scans were obtained with a resolution of 4 cm^{-1} within the wavelength range from 4000 to 550 cm^{-1}. The spectrum of each material was measured, averaged and corrected by background removal. Spectragryph V software was used to process the obtained spectra. 1.2.10 (Oberstdorf, Germany).

2.6.3. Thermal stability (TGA)

A thermogravimetric analyser (TA Instruments SDT 600, Warsaw, Poland) was used to measure the change in weight of the sample due to decoposition. During the measurement, the samples were heated at a constant rate of 10°C/min between 30°C and 800°C. The tests were conducted in a nitrogen atmosphere.

2.6.4. Mechanical properties and printability

The mechanical properties were tested using a universal testing machine (Instron model 5543 with "Merlin" V 4.42. software, Warsaw, Poland). Filaments were tested in accordance with ISO 527: 2012. The filaments were cut into 10 cm lengths and conditioned in an air climatic chamber at 25°C for 24 hours under relative humidity equal to 50%. In order to perform the measurement, each of the filaments was mounted in the jaws of the apparatus so that the length of the measurement section was 50 mm. The speed of the head movement causing the filament stretching was 100 mm/min. Each test was performed in 10 replicates. Based on the diagram of the relationship between breaking stress and deformation, test parameters such as tensile strength, strain at break and Young's modulus were determined. The printability of the filaments was assessed by the toughness parameter measurement in the indirect instrumental stiffness test proposed by Xu et others: kg/mm2*%, pressure unit expressed as a percentage and used to describe the mechanical parameters of tests using texture analysis methods (Xu et al., 2020). The universal testing machine

was equipped with a three-point-bending rig with thin blades (3 mm thickness). The filament was cut into 6 cm in length and placed on top of the machine platform. Trigger force was set to 50 g, and the blade was set to cut the filament until 1 mm in distance (57% strain) at a speed of 2 mm/s. The maximum force and fracture distance were recorded by Merlin software. Based on the area under the curve and maximum stress, the toughness parameter was calculated. The mechanical properties of the cylindrically shaped 3D prints were characterized according to the method described by Bi and Hoyer with co workers with slight modifications (Bi et al., 2011; Hoyer et al., 2012). Five cylindrical samples (Ø 12.5 mm h=20 mm) were compressed up to 10% deformation in two cycles at a test speed of 0.5 mm/s. The hardness, flexibility, and cohesiveness were measured. Hardness was determined as the ratio of the maximum force in the first compression cycle to the compressed surface. Elasticity is a dimensionless quantity expressed as the ratio of the distance of the pin compressing the sample from the beginning of compression to the achievement of the maximum force in the second cycle with the same distance determined in the first cycle. Cohesiveness, also a dimensionless value, was determined as the ratio of the area under the curve in the second compression cycle to the area under the curve in the first compression cycle.

2.6.5. Antimicrobial activity

The evaluation of antimicrobial properties of the materials was performed according to the ASTM E2149 method with slight modification using *E. coli* and *S. aureus* strains. Colonies of bacteria were first subcultured to triptic soya broth and incubated for 24 h at 37°C. Then microbial suspensions were diluted in phosphate buffered saline to obtain a number of bacterial cells between 1.5×10^7 to 5×10^7 CFU/mL. Dillutions were made with a spectrophotometer by measuring the absorbance at 600 nm wavelengths (optical density 0.08 ÷ 0.1). Antimicrobial activity tests were conducted for CS-CO_2/PVA composites, CS-CO_2/PVA/PCL filaments, and 3D prints.

To determine the antimicrobial activity of CS-CO_2/PVA composites, squares with 5 cm edge length were cut out of the composites and PE film (negative control without the antimicrobial properties). Then square samples were sterilised under UV radiation (30 minutes on each side). Afterwards, 0.4 mL of inoculum containing 1.5×10^7 to 5×10^7 CFU/mL of tested bacterial strain was applied to each of the square. The inoculated samples were covered with sterile square-shaped PE foils with an edge length of 4 cm to ensure proper contact of the bacterial suspension with the tested material (16 cm^2). The samples prepared in this way were incubated 24 hours at 37°C (Heidolph Incubator 1000, Merck Sp. z o.o., Warsaw, Poland). After incubation each sample was transferred to 10 mL PBS solution and shaken 5 times for 5 seconds each using a vortex. Ten-fold dilutions of PBS extracts in peptone water were made ($10^0 \div 10^8$) and inoculations on TSA medium by flooding. The plates were incubated at 37°C for 24 hours. After the incubation, bacterial colonies that grew on Petri plates were counted.

For determination of antimicrobial activity of filaments, cell suspensions containing 1.5×10^7 to 5×10^7 CFU/mL of tested bacterial strain, were placed in separate bottles of 45 mL, followed by addition of 5 g of PCL filament (control sample) or proper CS-CO_2/PVA/PCL filament (tested sample). Then samples were incubated at 37°C for 24 hours in an incubator with constant shaking at 200 rpm (Heidolph Unimax 1010, Merck Sp. z o.o., Warsaw, Poland). After incubation, ten-fold dilutions in peptone water were made ($10^0 \div 10^8$) and inoculations on TSA medium by flooding. The

plates were incubated at 37°C for 24 hours. After the incubation, bacterial colonies that grew on Petri plates were counted.

The antimicrobial activity of the 3D prints was evaluatedanalogously to the procedure used for CS-CO_2/PVA composites. The test samples were prepared by printing the tiles in a square shape. with a side length of 5 cm and a thickness of 0.5 cm. The negative control was a plaque of the same dimensions printed from PCL.

To calculate the number of cells per mL of the initial suspension, the results of the colony counts were used, the number of which, after incubation on the plates, ranged from 30 ÷ 300 units, according to the equation:

$$Vc = N \times D,$$

where Vc is the bacteria concentration, in colony forming units per ml (CFU/mL),N is the average value, in colony forming units (CFU), from Petri dishes, D is the dilution factor from the plates counted. Antimicrobial activity was calculated according to the formula:

$$R = \log\frac{B}{C},$$

where B is the average of the number of viable cells on the tested sample after 24 h incubation at 37°C (CFU/mL), C is the average of the number of viable cells on the control sample after 24 h incubation at 37°C (CFU/mL). A percentage reduction of bacteria/fungi on a logarithmic scale (R) equal to 1, 2, and 3 corresponds to a reduction of 90%, 99%, and 99.9%, respectively.

2.7. Statistical Analysis of the Data

The STATISTICA software (StatSoft, Inc., Tulsa, OK, USA) was used for analyses. The statistical significance was determined at $p < 0.05$. All data reported were based on the means of three replicates ($n = 3$) or five (n=5) replicates in the case of mechanical tests. Experimental results were expressed as mean ± standard deviation (SD). Student's t-test and one-way analysis of variance (ANOVA) were applied. The differences were considered to be statistically significant at $p < 0.05$.

3. Results and discussion

3.1 Assessment of the effect of temperature treatment on the stability of CS-CO_2/PVA composites

During visual evaluation of the influence of temperature treatment on the stability of CS-CO_2/PVA composites, significant differences in their colour were observed. They resulted from the type of acid used during composites preparation (Fig.1).

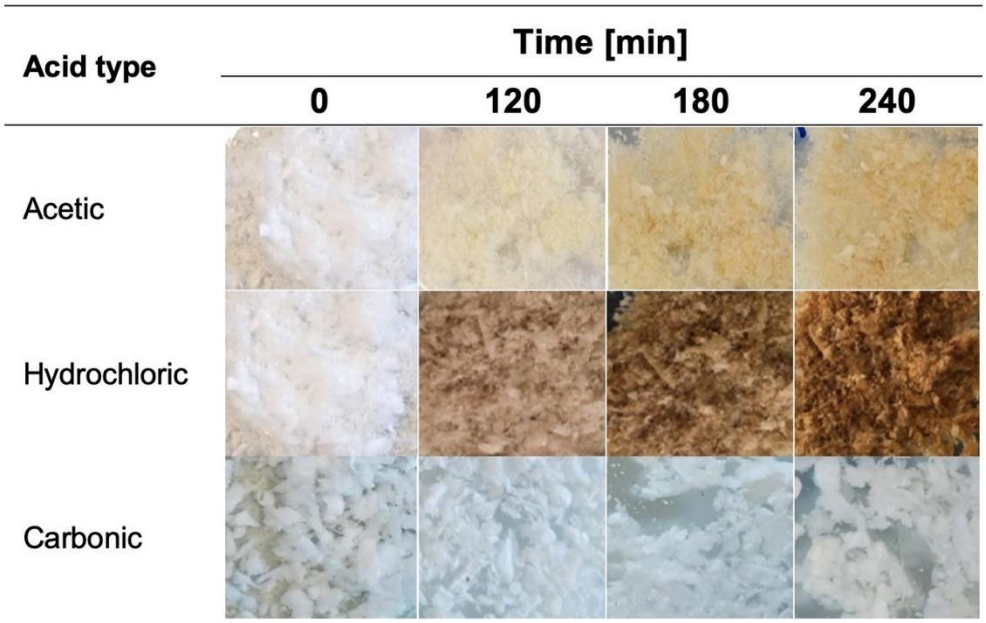

Fig.1. Comparison of color changes of CS-CO_2/PVA composites at the ratio of 1:1 m/m heated at 150°C for 4 hours.

The change in the colour of samples indicated the degradation of polymers present in the composite. It is an undesirable phenomenon as it leads to structural changes in polymer chains (e.g. loss of molecular weight) and as a result, changes in the physicochemical and biological properties of the material. In the context of the use of chitosan in various biomaterials, the greatest threats are biodegradation, degradation by ultrasounds, thermal degradation, and photodegradation. The presence of acid in chitosan materials mainly causes the hydrolysis of the polymer to a lower molecular weight without significantly affecting the deacetylation degree and polydispersity (Sikorski, Gzyra-Jagieła, & Draczyński, 2021). The strongest darkening of the composites was observed while using hydrochloric acid. During four hours of heating at 150°C, the colour changed from white to brown. A less intense colour change during heating was shown in the material for which a solution of chitosan in acetic acid was used. After heating this material under the same conditions a change in colour from white to yellow was observed. In the case of composites prepared with chitosan solution in carbonic acid, no effect of temperature on the change of their colour was observed. Grande and co-workers found that the color change of CS/PVA blends is dependent on the drying method, and best results can be obtained by using freeze-drying and spray-drying (an only slightly yellow tone) (Grande et al., 2018). However, subjecting thus dried composites containing at least 25% (m/m) of chitosan to hot-pressing (150°C), still causes their darkening, even if volatile acetic acid was used to dissolve chitosan. Hot-pressed composites did not change their color due to the temperature treatment, when the chitosan content in their composition did not exceed 10% (m/m). The results we presented confirmed that the innovative method of dissolving chitosan with the use of carbon dioxide allowed the creation of thermostable CS-CO_2/PVA composites, even if chitosan constitutes as much as 50% of their mass.

3.2. CS-CO_2/PVA chemical structure

The infrared spectroscopy was used to identify individual chemical groups in pure chitosan and PVA as well as to register structural changes in composites of both polymers (Fig. 2). Figure 2.A shows the chitosan spectrum. Intense signals at wavelengths of 1150 cm^{-1}, 1058 cm^{-1}, 1026 cm^{-1} and 893 cm^{-1} indicate the presence of a saccharide structure. Another characteristic band at 3349/3301 cm^{-1} is the signal coming from the hydroxyl group of the chitosan molecule. A series of signals at 1652 cm^{-1}, 1557 cm^{-1} and 1315 cm^{-1} correspond to amides I, II and III. The remaining marked signals come from groups -CH_2- (Mania et al., 2019; Staroszczyk, Sztuka, Wolska, Wojtasz-Pająk, & Kołodziejska, 2014).

The PVA spectrum is shown in Figure 2.B. Both PVA and chitosan spectra have several analog signals. The signal at about 3342 cm^{-1} corresponds to tensile vibrations of the hydroxyl group, at 2917 cm^{-1} and 1426 cm^{-1} to tensile and deformation vibrations of alkyl grups. Other signals characteristic for PVA are in the range 1750-1000 cm^{-1}. For example, the band at 1726 cm^{-1} is a signal of C-O and C=O tensile vibrations of the acetate group. In addition, several signals have been observed which are the result of interactions between PVA mers such as at 1371 cm^{-1} ((OH)-C-OH), 1238 cm-1 (=C-O-C), 1088 cm^{-1} (C-O-C) and 1020 cm^{-1} ((C-O)-C-OH) (Alhosseini et al., 2012; Mansur, Sadahira, Souza & Mansur, 2008).

Analyzing the spectrum of PVA/CS composites (Figure 2.C), characteristic peaks were detected as in the spectra of individual components of this composite. Chitosan and PVA do not show strong interactions between each other as evidenced by the lack of new signals and significant shifts of existing peaks. The only shift observed was found in the case of signals corresponding to tensile vibrations of hydroxyl and alkyl groups. Moreover, on the basis of the obtained spectrum it was confirmed that the intensity of its signals increases with the increase of the share in the composition of a given polymer. These results are consistent with the work of Grande and co-workers (Grande et al., 2018).

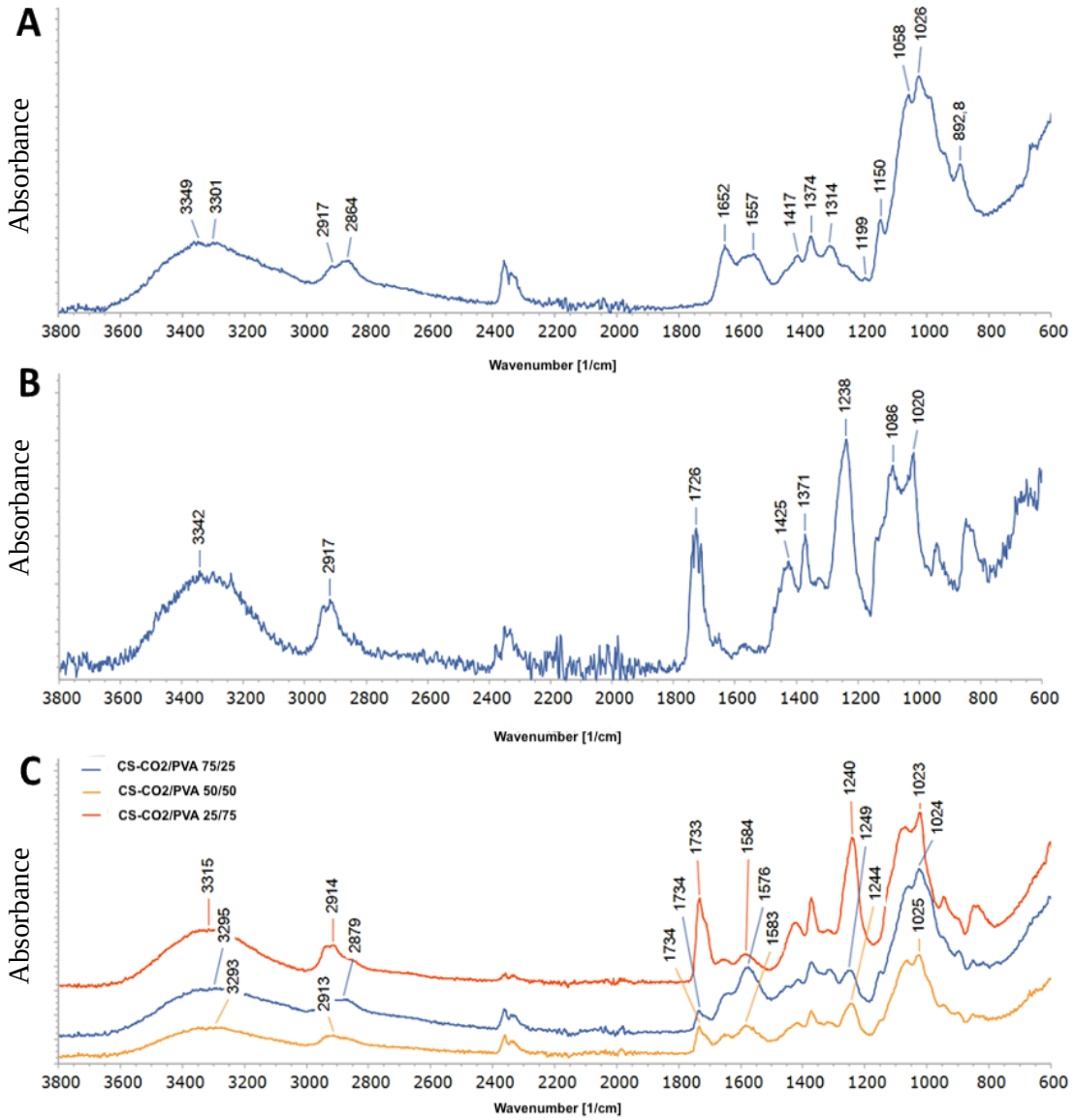

Fig.2. FTIR spectra obtained for CS (A), PVA (B) and PVA/CS (C) composites.

3.3. CS-CO_2/PVA/PCL filaments production

PCL was used as the matrix for the production of filaments and doped with one of the three CS-CO_2 /PVA obtained composite. The 1% solutions of CS-CO_2 and PVA were combined to obtain CS-CO_2/PVA composites with mass fractions of 75/25, 50/50 and 25/75. The freeze-dried composites subesquently subjected to extrusion are shown in Figure 3.

Fig. 3. Granules obtained by combining CS-CO_2 and PVA solutions, freeze drying and extrusion (150°C) at mass ratios 25/75 (A), 50/50 (B) and 75/25 (C).

Filaments obtained by extrusion PCL with 20% addition of CS-CO_2 composite are shown in Figure 4.

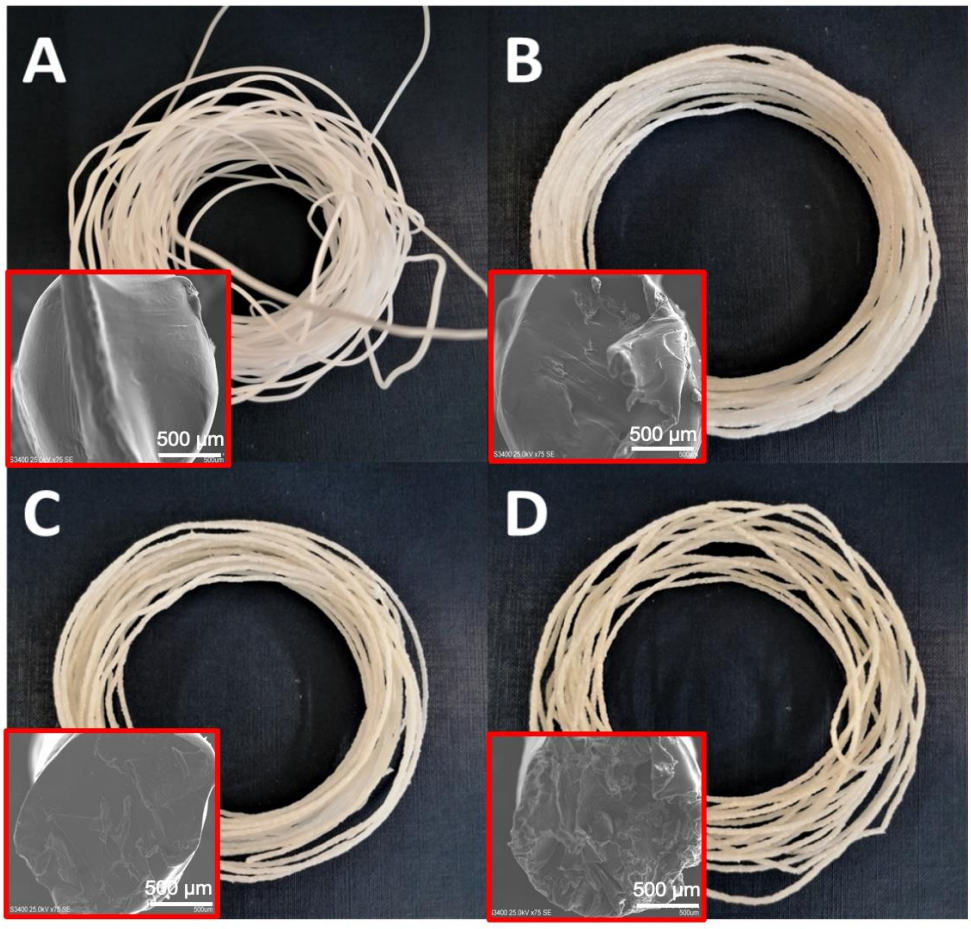

Fig. 4. Photographs and SEM micrographs of CS-CO_2/PVA/PCL filaments at mass ratios: 0/0/100 (A), 5/15/80 (B), 10/10/80 (C), 15/5/80 (D).

Based on SEM micrographs, it was observed that the filaments became less homogeneous with increasing chitosan concentration. They have a more coarser structure compared to the filament obtained exclusively from PCL granules. The increase in filament heterogeneity with the increase in chitosan concentration was also observed in our previous work, where PLA was used as the base

thermoplastic material. Due to the lack of the compatibilizer in the form of PVA, the deposition of chitosan in the PLA matrix resulted in the formation of large pores in the filament and air pockets, when the chitosan concentration was 10% (Mania et al., 2019). The use of PVA prevents such problems, even when chitosan constitutes 15% of the filament's weight. Grande et al (2015) demonstrated that the use of freeze-drying in the formation of PVA/chitosan composites significantly improves the dispersion of these composites in PLA. The evidence is the observed particle size distribution and a reduction in the dispersed particle reaching 0.5–5 μm during the thermomechanical mixing process, as demonstrated by the SEM analysis (Grande et al., 2015). In our investigation we observed that increase of the chitosan content in CS-CO_2/PVA composite caused the worst distribution and the worst homogenity of the material. For CS-CO_2/ PVA composite containing 25%, 50%, and 75% of chitosan (m/m), the particle distribution was in the range 5 -10 μm, 25 - 40 μm, and 50 - 60 μm, respectively (*Supplementary materials*). Chen and colleagues suggested that particle distribution is associated with hydrogen bonds between the hydroxyl groups of PVA and the amino groups of chitosan. Increasing the chitosan content in the material increases the the level of ionic cross-linking tended to form the bigger CS/PVA particle agglomerates (Chen et al., 2017). This understanding matches the results obtained for filaments using the SEM technique (Fig. 4).

3.4. Thermal stability

The thermograms, derivative weight plots of CS-CO_2/PVA/PCL and their components are presented in figure 5. The TGA curve of chitosan exhibited an endothermic effect attributable to water release at the range 25-145°C (Fig. 5A) with 13.1% weight loss. The second decomposition stage is attributed to a complex process including dehydratation of saccharide rings, depolymerization and decomposition of the acethylated units of the polymer (42.0% weght loss) (Lewandowska, 2009; Moussout, Ahlafi, Aazza & Bourakhouadar, 2016). According to Eulalio and others, the third decomposition stage (measured for chitosan powder) is a thermo-oxidative process that starts at approx. 500°C, with maximum velocity at approx. 600°C and a weight loss of 40-45%, leaving no residue behind (Eulalio, Rodrigues, Santos, Peniche, & LiaFook, 2019) . In our tests, there was also a loss in weight that occurred above 400°C continuously with a small offset at 740°C (Fig.5A). The PVA curve consisted of three stages (Fig. 5B). The first weight loss at 20-120°C is related to moisture vaporization (4% weight loss). The second occurs at 305°C with 75% weight loss due to dehydration of the chain with the release of volatile compounds. The last stage of weight loss above 400°C is caused by degradation of polyene residues with formation of carbon and hydrocarbon (Lewandowska, 2009; Raju, Rao, Reddy, & Veera Brahmam, 2007). The TGA curve of PCL shows only one stage of mass loss due to the lack of water absorption capacity of this polymer. In the temperature range from 350°C to 420°C almost complete weight loss due to depolymerization with the formation of ε-caprolactone, which is subject to further decomposition is observed (Aoyagi, Yamashita, & Doi, 2002). In turn, the TGA curves of CS-CO_2/PVA/PCL filaments were characterized by only one stage of decomposition, during which almost complete loss of mass occurred (Fig. 5.D-F). Both the curve course and the temperature value range for the stage of greatest mass loss coincide with the TGA PCL curve. The results of the thermal analysis confirm the results of the visual assessment of the CS-CO_2/PVA composites (Fig. 1). The PCL degradation starts above 350°C, so any loss of filament

weight until the printing temperature is reached may result from changes in chitosan and PVA. However, the weight loss of all produced filaments up to 150°C did not exceed 2% which suggests that the composites do not absorb nearly as much water as the CS and PVA materials. (Fig. 5 D-F). The weight loss measured up to 150°C for chitosan, PVA and CS-CO_2/PVA composites containing 25%, 50% and 75% chitosan, was 18%, 5%, 5%, 7%, 10%, respectively. Thermograms for CS-CO_2/PVA composites are found in the *Supplementary materials* file. The decomposition temperature of them appears to shift from 275°C towards 225°C with increasing CS content. This is above the extrusion and printing temperature of 150°C, but is consistent with decomposition temperatures of 275°C for PVA and 225°C for CS.

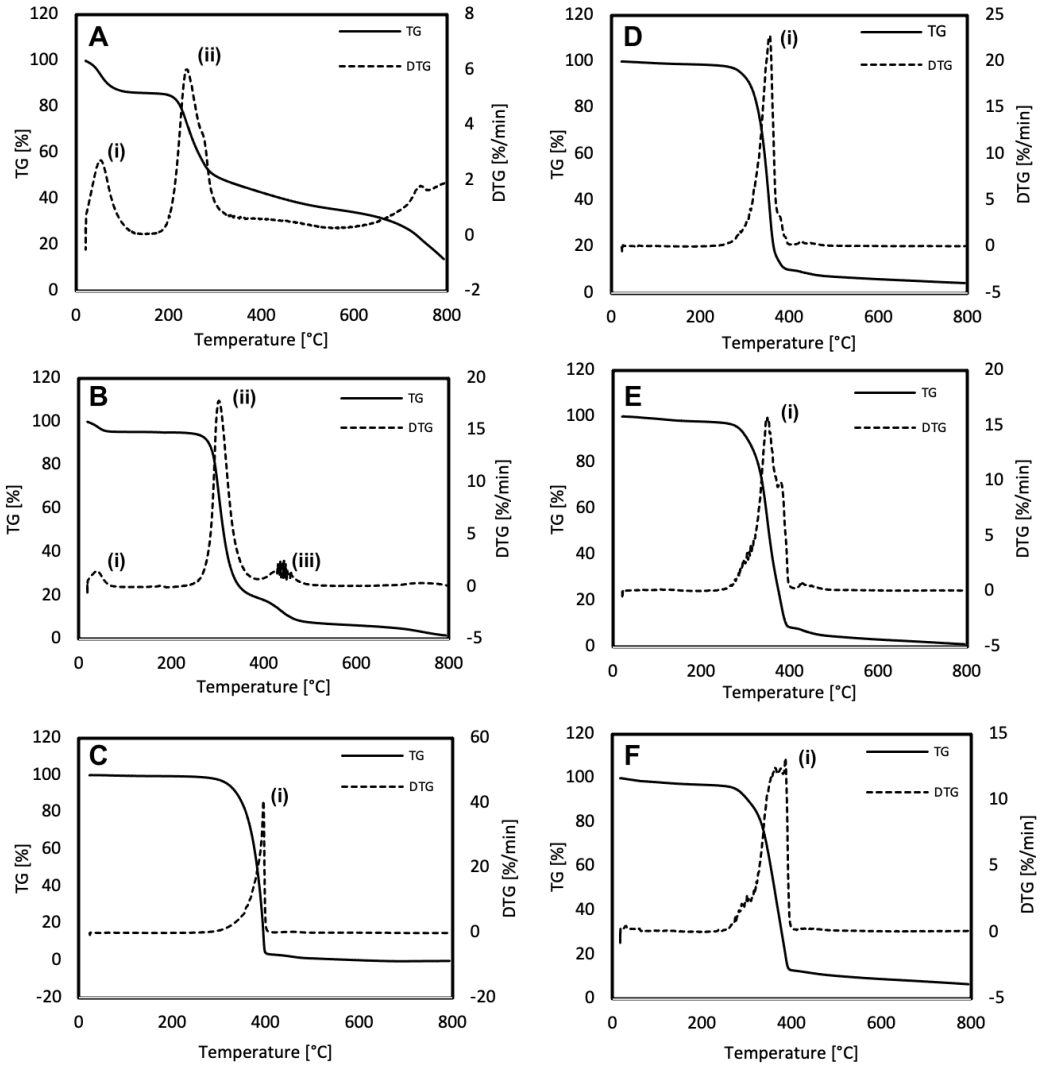

Fig. 5. TGA and TGA derivative curves of chitosan (A) CS, (B) PVA, (C) PCL, (D) CS-CO_2/PVA/PCL filament with 5/15/80 components ratio, (E) CS-CO_2/PVA/PCL filament with 10/10/80 components ratio, (F), CS-CO_2/PVA/PCL filament with 15/5/80 components ratio.

3.5. Mechanical properties and printability

The comparison of the filaments printability, mechanical properties of filaments and 3D prints obtained from them are presented in Table 1. The obtained CS-CO_2/PVA/PCL filaments were subjected to

mechanical tensile tests to determine the following parameters: tensile strength, elongation at break and Young's modulus. Based on the obtained results, significant differences between pure PCL and subsequent CS-CO_2/PVA/PCL samples with different chitosan content were found. The addition of the filler in the form of the CS-CO_2/PVA composite decreased the tensile strength by 73.6%, 67.8% and 56.6%, in relation to the PCL value, when the chitosan content in the filament was 5%, 10% and 15%, respectively. Filaments containing chitosan had 50-64% lower extension at break value and 50-75% lower Young modulus than the PCL filament. Deterioration of the mechanical properties of filaments with an increase in chitosan concentration was also observed in our previous work (Mania et al., 2019). Reduction in tensile strength by about 60% in PLA filaments with addition of 10% chitosan corresponded to the same reduction in tensile strength of CS-CO_2/PVA/PCL filaments with a 15/5/80 ratio. The equal reduction in tensile strength even at 5% higher concentration of chitosan in thermoplastic filaments may be due to the use of PVA as a compatibilizer in the physical mixture of raw materials. Filaments containing a filler in the form of a composite of chitosan with PVA, in relation to filaments only with the addition of chitosan, but at a similar concentration of this polymer, are characterized by lower elongation ability (Mania et al., 2019). Based on Young modulus-tensile strength chart, all obtained CS-CO_2/PVA/PCL filaments are classified as natural materials (Shah, 2014). Properties closest to thermoplastic materials were demonstrated by a filament with addition of 15% chitosan. To be included in this group, the same filament should have approx. 2.7 times greater tensile strength with recent Young modulus.

Despite the significant deterioration of the mechanical parameters of the filaments resulting from the use of the CS-CO_2/PVA composite filler in the PCL matrix, all filaments obtained can be described as printable. They fall within the printability window described in the experiment of Xu and colleagues: > 80 kg/mm^2*% (Xu et al., 2020). The printability of the filaments demonstrated in the instrumental test was confirmed in a printout using a 3D FDM printer (Fig.6).

Table 1. Comparison of the filaments' printability, their mechanical properties and 3D prints obtained from them (n=10, p<0.05).

Material type	PCL	CS-CO_2/PVA/PCL 5/15/80	CS-CO_2/PVA/PCL 10/10/80	CS-CO_2/PVA/PCL 15/5/80
		Filament		
Tensile strength [MPa]	21.49 ± 1.02^a	5.68 ± 0.15^b	6.91 ± 0.21^c	9.32 ± 0.43^d
Extension at break [%]	21.96 ± 0.79^a	10.89 ± 0.30^b	10.34 ± 0.44^b	7.83 ± 0.19^c
Young modulus [MPa]	15.50 ± 0.48^a	8.03 ± 0.50^b	6.22 ± 0.18^c	3.98 ± 0.09^d
Printability [kg/mm^2*%]	187.9 ± 3.2^a	131 ± 2.0^b	103.1 ± 1.4^c	95.3 ± 1.1^d
		3D print		
Hardness [kPa]	3.42 ± 0.08^a	3.95 ± 0.06^b	4.35 ± 0.09^c	4.67 ± 0.04^d
Flexibility [-]	0.88 ± 0.03^a	0.72 ± 0.05^b	0.69 ± 0.03^b	0.57 ± 0.02^c
Cohesiveness [-]	0.73 ± 0.05^a	0.70 ± 0.04^a	0.62 ± 0.06^a	0.65 ± 0.02^a

Values with different letters marked from a to d differ significantly fromthe control sample in each row.

Compression tests have shown that increasing the chitosan concentration in the printout increases its hardness and decreases and its flexibility. The samples with addition of 5%, 10% and 15% chitosan were 15.5%, 27.2% and 36.5% harder and 18.2%, 21.6% and 35.2% less flexible compared to PCL,respectively. The addition of chitosan did not significantly affect the cohesiveness of the 3D prints, which was comparable to that of the prints made of polycaprolactone (Table 1). Visually, there was no difference between the samples.

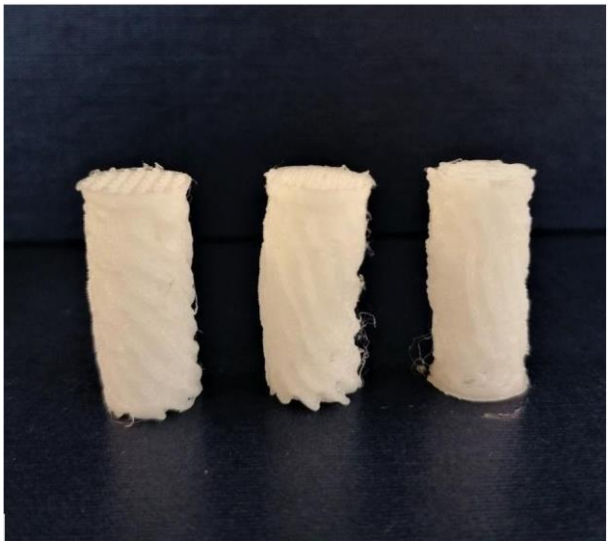

Fig.6. The photography of 3D objects in the form of cylinders printed with the FDM method from the obtained composite filaments (from the left 3D prints containinng 5%, 10% and 15% of chitosan).

3.6. Antimicrobial properties

To evaluate the antimicrobial properties of the filaments the ASTM: E2149 method with slight modifications was used, which is designed to measure the antimicrobial activity of non-leaching (non-water soluble) antimicrobials surfaces made of plastic, rubber, silicone, and treated fabric material and is one method to test an irregularly shaped antimicrobial object, such as a thread, powder or 3D molded plastic. The results of the antimicrobial activity tests are presented in the form of the degree of reduction obtained after 24-hour contact of *S. aureus* and *E.coli* inoculum with the tested materials. PCL and PVA have no antimicrobial properties (Aslam, Kalyar, & Raza, 2018; Balcucho, Narváez, & Castro-Mayorga, 2020). It was found that all CS-CO_2/PVA composites had the strongest antimicrobial effect against *S. aureus* and *E. coli (*at least 2 log orders which corresponds to 99% reduction*),* compared to PCL filaments and prints. This activity also increased for both bacterial strains along with an increase in chitosan concentration in the material (Fig.7.) The highest value was recorded for CS-CO_2/PVA composites containing 75% of chitosan against a *S. aureus* strain. The same composite also caused the strongest antimicrobial effect after being used to produce filaments and for 3D printing. The greater antimicrobial effect of the CS-CO_2/PVA composite, CS-CO_2/PVA/PCL filaments and 3D prints was obtained with respect to the Gram-positive strain. The 3D prints showed virtually the same antimicrobial properties as the filaments from which they were printed. It means that re-melting the CS-CO_2/PVA/PCL material has no significant effect on the inhibition of the material's antimicrobial activity. The antimicrobial activity was due to the presence of chitosan and depends on the degree of its deacetylation, molecular weight, concentration in solution, pH, and ionic strength of the solution (Rinaudo, 2006). According to Goy and colleagues, there is a lack of conclusive data on whether chitosan has higher activity on Gram-positive or on Gram-negative bacteria (Goy, de Britto, & Assis, 2009). On both strains, chitosan seems to act differently, though in both cases satisfactorily. The main reason for the antimicrobial activity of chitosan is the interaction of its positively charged chains with anionic components of microorganisms—lipopolysaccharides (Gram-negative bacteria) and teichoic acids

(Gram-positive bacteria) that cause bacterial cell lysis. However, this mechanism takes place when the amino groups of the polymer are protonated: pH < 6 (Kong, Chen, Xing, & Park, 2010).

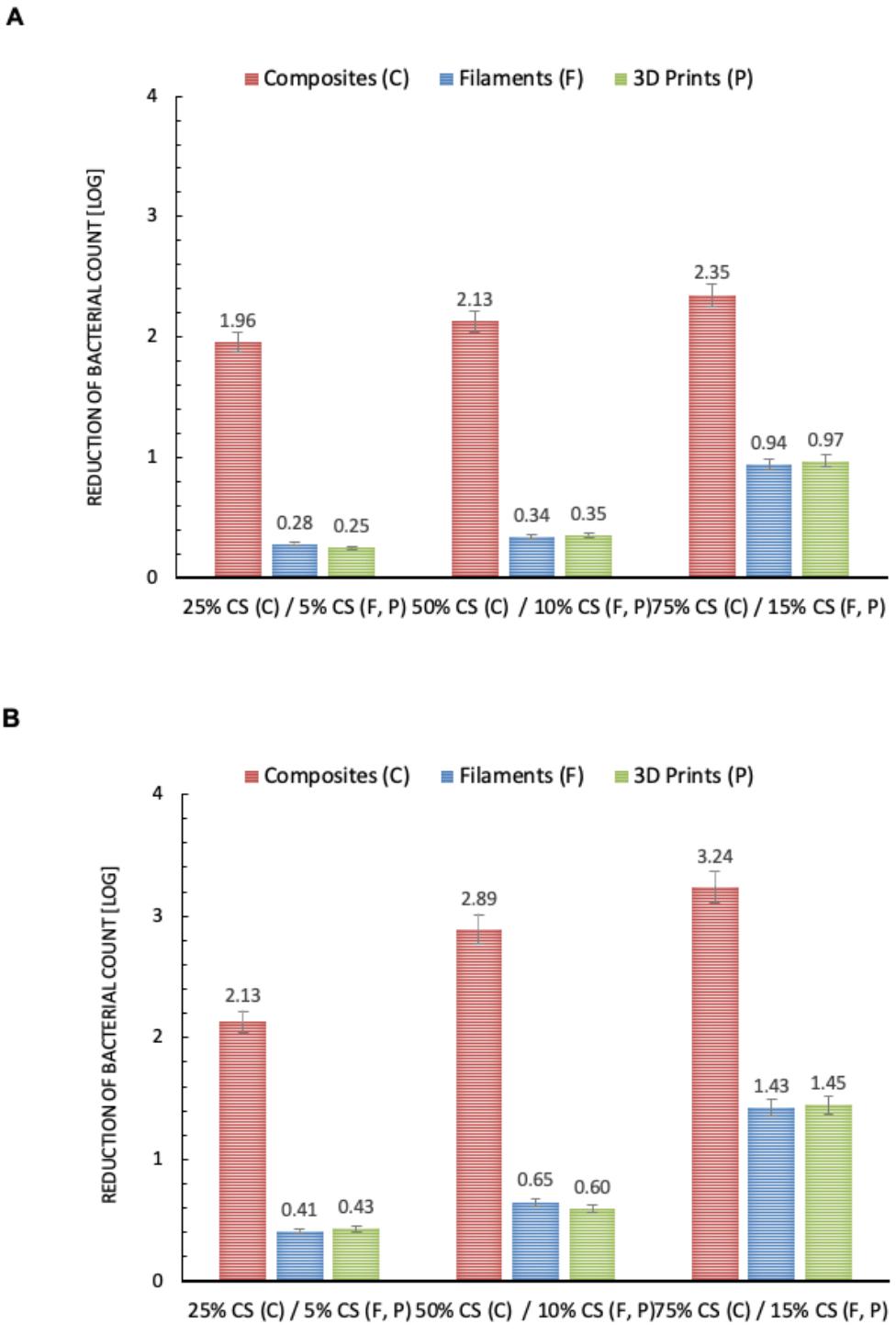

Fig. 7. The antimicrobial activity against (A) *E. coli* and (B) *S.aureus* of CS-CO_2/PVA composites, and CS-CO_2/PVA/PCL filaments and prints estimated according to Standard ASTM: E2149.

It has been concluded that for neutral or alkaline media, the cationic nature of chitosan can no longer explain its antibacterial activity. In this case, the strong coordination capability of –NH_2

groups in the chitosan chain might be one possible mechanism (Mania et al., 2018; Xie, Wang, & Liu, 2002).

In the scientific literature, it has been confirmed that the antimicrobial activity of chitosan does not imply a cytotoxic effect. Da Silva and co-workers used chitosan from the same producer and with the same parameters to obtain scaffolds for cartilage tissue engineering. They confirmed that the viability of the chondrocytes from pig stifles estimated by the live / dead assay did not differ between the four groups of chitosan scaffolds and was above 80% (Da Silva et al., 2016). Moreover, in the earlier work of our team it was shown that chitosan hydrogels obtained by the CO_2 saturation method are characterized by higher biocompatibility towards mouse NIH 3T3 fibroblasts, than their counterparts in solutions of organic or mineral acids (Gorczyca et al., 2014). Also no cytotoxic effect was noted for polycaprolactone and polyvinyl alcohol (Ragetly et al., 2010; Zhang et al., 2019)

4. Conclusion

In our work we present an innovative method for processing chitosan in a thermoplastic matrix.The use of the CO_2 saturation technique in the preparation of CS-CO_2/PVA composites allows generation of a polar filler for thermoplastics containing up to 75% chitosan. So far, such a solution has not been presented by any research team and it overcame the limitation previously described in the literature regarding the presence of residual solvents. The use of a 20% filler addition in a thermoplastic material allows it to achieve a chitosan concentration in the range of 5-15% m / m, and to produce a filament suitable for use in 3D printing with the FDM technology. Both, CS-CO_2/PVA/PCL filaments and prints are characterized by antimicrobial activity against gram negative and gram positive indicator bacteria. This activity depends on the concentration of chitosan and ensure reduction of bacterial growth even above 0.94 in logarithmic scale (89%) in the case of materials containing 15% of chitosan. The filler decreases the mechanical properties of the filaments, but it does not significantly affect their printability. On the other hand, 3D prints become harder, less flexible and consistent with increasing chitosan concentration. The absence of acid in the materials allows the thermal stability of the filaments to be ensured, which is extremely important in its further processing, including in 3D printing conditions.The presented results may have great potential in biological applications as cell growth scaffolds, including in regenerative medicine.

Author Contributions:

Conceptualization: R.T, S.M., Data curation, S.M., P.K., A.B-K., and R.T.; Formal analysis, R.T. and S.M,; Funding acquisition, R.T. and S.M. Investigation, R.T, P.K. and S.M.; Methodology, R.T., P.K. and S.M.; Project administration, R.T. and S.M.; Resources, R.T., P.K., A.B-K. and S.M.; Software, R.T., P.K., A.B-K. and S.M Supervision, R.T. and S.M.; Validation,R.T., A.B-K. and S.M.; Visualization, R.T., P.K., A.B-K., and S.M.; writing—original draft preparation, R.T., P.K., A.B-K., and S.M.; writing—review and editing, R.T., P.K., A.B-K., and S.M. All authors have read and agreed to the published version of the manuscript.

Funding: This research was supported by the internal minigrant No 035153 funded by Dean od Chemical Faculty of Gdansk University of Technology in 2021.

Acknowledgments: The authors would like to thank Professor Piotr Bruździak for his help in preparing FTIR spectra (Department of Physical Chemistry, Faculty of Chemistry, GUT) and Dr Timothy E.L. Douglas for the linguistic proofreading of the publication (Engineering Department, Lancaster University, UK).

Conflicts of Interest: The authors declare no conflict of interest.

References

Alhosseini, S. N., Moztarzadeh, F., Mozafari, M., Asgari, S., Dodel, M., Samadikuchaksaraei, A., Kargozar, S., & Jalali, N. (2012). Synthesis and characterization of electrospun polyvinyl alcohol nanofibrous scaffolds modified by blending with chitosan for neural tissue engineering. *International Journal of Nanomedicine*, *7*, 25–34.

Aoyagi, Y., Yamashita, K., & Doi, Y. (2002). *Thermal degradation of poly [(R) -3-hydroxybutyrate], poly [e -caprolactone], and poly [(S) -lactide]*. *76*, 53–59.

Aslam, M., Kalyar, M. A., & Raza, Z. A. (2018). Polyvinyl alcohol: A review of research status and use of polyvinyl alcohol-based nanocomposites. *Polymer Engineering & Science*, *58*, 2119–2132.

Balcucho, J., Narváez, D. M., & Castro-Mayorga, J. L. (2020). Antimicrobial and biocompatible polycaprolactone and copper oxide nanoparticle wound dressings against methicillin-resistant staphylococcus aureus. *Nanomaterials*, *10*(9), 1–21. https://doi.org/10.3390/nano10091692

Bi, L., Cao, Z., Hu, Y., Song, Y., Yu, L., Yang, B., Mu, J., Huang, Z., & Han, Y. (2011). Effects of different cross-linking conditions on the properties of genipin-cross-linked chitosan/collagen scaffolds for cartilage tissue engineering. *Journal of Materials Science: Materials in Medicine*, *22*(1), 51–62. https://doi.org/10.1007/s10856-010-4177-3

Bonilla, J., Fortunati, E., Vargas, M., Chiralt, A., & Kenny, J. M. (2013). *Accepted Manuscript*.

Chen, Q., Liu, Y., Wang, T., Wu, J., Zhai, X., Li, Y., Lu, W. W., Pan, H., & Zhao, X. (2017). Chitosan-PVA monodisperse millimeter-sized spheres prepared by electrospraying reduce the thromboembolic risk in hemorrhage control. *Journal of Materials Chemistry B*, *5*(20), 3686–3696. https://doi.org/10.1039/c7tb00032d

Correlo, V. M., Boesel, L. F., Pinho, E., Costa-Pinto, A. R., Alves Da Silva, M. L., Bhattacharya, M., Mano, J. F., Neves, N. M., & Reis, R. L. (2009). Melt-based compression-molded scaffolds from chitosan-polyester blends and composites: Morphology and mechanical properties. *Journal of Biomedical Materials Research - Part A*, *91*(2), 489–504. https://doi.org/10.1002/jbm.a.32221

Da Silva, A. R. P., Macedo, T. L., Coletta, D. J., Feldman, S., & Pereira, M. de M. (2016). Synthesis, characterization and cytotoxicity of Chitosan/Polyvinyl alcohol/bioactive glass hybrid scaffolds obtained by Lyophilization. *Revista Materia*, *21*(4), 964–973. https://doi.org/10.1590/S1517-707620160004.0089

Dang, K. M., & Yoksan, R. (2015). Development of thermoplastic starch blown film by incorporating plasticized chitosan. *Carbohydrate Polymers*, *115*, 575–581. https://doi.org/10.1016/j.carbpol.2014.09.005

Epure, V., Griffon, M., Pollet, E., & Avérous, L. (2011). Structure and properties of glycerol-plasticized chitosan obtained by mechanical kneading. *Carbohydrate Polymers*, *83*(2), 947–952. https://doi.org/10.1016/j.carbpol.2010.09.003

Eulalio, H. Y. C., Rodrigues, J. F. B., Santos, K. O., Peniche, C., & LiaFook, M. V. (2019). Characterization and. thermal properties of chitosan films prepared with different acid solvents. *Revista Cubana de Química*, *31*, 309–323.

Gorczyca, G., Tylingo, R., Szweda, P., Augustin, E., Sadowska, M., & Milewski, S. (2014). Preparation and characterization of genipin cross-linked porous chitosan-collagen-gelatin scaffolds using chitosan-CO_2 solution. *Carbohydrate Polymers*, *102*(1), 901–911. https://doi.org/10.1016/j.carbpol.2013.10.060

Goy, R. C., De Britto, D., & Assis, O. B. G. (2009). A review of the antimicrobial activity of chitosan. *Polimeros*, *19*(3), 241–247. https://doi.org/10.1590/S0104-14282009000300013

Grande, R., Pessan, L. A., & Carvalho, A. J. F. (2015). Ternary melt blends of poly(lactic acid)/poly(vinyl alcohol)-chitosan. *Industrial Crops and Products*, *72*, 159–165.

Grande, R., Pessan, L. A., & Carvalho, A. J. F. (2018). Thermoplastic blends of chitosan: A method for the preparation of high thermally stable blends with polyesters. *Carbohydrate Polymers*, *191*(December 2017), 44–52. https://doi.org/10.1016/j.carbpol.2018.02.087

Hoyer, B., Bernhardt, A., Heinemann, S., Stachel, I., Meyer, M., & Gelinsky, M. (2012). Biomimetically mineralized salmon collagen scaffolds for application in bone tissue engineering. *Biomacromolecules*, *13*(4), 1059–1066. https://doi.org/10.1021/bm201776r

Kong, M., Chen, X. G., Xing, K., & Park, H. J. (2010). Antimicrobial properties of chitosan and mode of action: A state of the art review. *International Journal of Food Microbiology*, *144*(1), 51–63. https://doi.org/10.1016/j.ijfoodmicro.2010.09.012

Lewandowska, K. (2009). Miscibility and thermal stability of poly(vinyl alcohol)/chitosan mixtures. *Thermochimica Acta*, *493*(1–2), 42–48. https://doi.org/10.1016/j.tca.2009.04.003

Mania, S., Ryl, J., Jinn, J.-R., Wang, Y.-J., Michałowska, A., & Tylingo, R. (2019). The production possibility of the antimicrobial filaments by co-extrusion of the pla pellet with chitosan powder for FDM 3D printing technology. *Polymers*, *11*(11). https://doi.org/10.3390/polym11111893

Mania, S., Tylingo, R., Augustin, E., Gucwa, K., Szwacki, J., & Staroszczyk, H. (2018). Investigation of an elutable N-propylphosphonic acid chitosan derivative composition with a chitosan matrix prepared from carbonic acid solution. *Carbohydrate Polymers*, *179*. https://doi.org/10.1016/j.carbpol.2017.09.082

Mania, Szymon, Banach, A., & Tylingo, R. (2020). Review of current research on chitosan as a raw material in three-dimensional printing technology in biomedical applications. *Progress on Chemistry and Application of Chitin and Its Derivatives*, *25*, 37–50. https://doi.org/10.15259/PCACD.25.003

Mansur, H. S., Sadahira, C. M., Souza, A. N., & Mansur, A. A. P. (2008). FTIR spectroscopy characterization of poly (vinyl alcohol) hydrogel with different hydrolysis degree and chemically crosslinked with glutaraldehyde. *Materials Science and Engineering C*, *28*(4), 539–548. https://doi.org/10.1016/j.msec.2007.10.088

Matet, M., Heuzey, M. C., Pollet, E., Ajji, A., & Avérous, L. (2013). Innovative thermoplastic chitosan obtained by thermo-mechanical mixing with polyol plasticizers. *Carbohydrate Polymers*, *95*(1), 241–251. https://doi.org/10.1016/j.carbpol.2013.02.052

Mendes, J. F., Paschoalin, R. T., Carmona, V. B., Sena Neto, A. R., Marques, A. C. P., Marconcini, J. M., Mattoso, L. H. C., Medeiros, E. S., & Oliveira, J. E. (2016). Biodegradable polymer

blends based on corn starch and thermoplastic chitosan processed by extrusion. *Carbohydrate Polymers*, *137*, 452–458. https://doi.org/10.1016/j.carbpol.2015.10.093

Moussout, H., Ahlafi, H., Aazza, M., & Bourakhouadar, M. (2016). Kinetics and mechanism of the thermal degradation of biopolymers chitin and chitosan using thermogravimetric analysis. *Polymer Degradation and Stability*, *130*, 1–9. https://doi.org/10.1016/j.polymdegradstab.2016.05.016

Muzzarelli, R. A. A. (2009). Chitins and chitosans for the repair of wounded skin, nerve, cartilage and bone. *Carbohydrate Polymers*, *76*(2), 167–182. https://doi.org/10.1016/j.carbpol.2008.11.002

Ngo, T. D., Kashani, A., Imbalzano, G., Nguyen, K. T. Q., & Hui, D. (2018). Additive manufacturing (3D printing): A review of materials, methods, applications and challenges. *Composites Part B: Engineering*, *143*(December 2017), 172–196. https://doi.org/10.1016/j.compositesb.2018.02.012

Ragetly, G. R., Slavik, G. J., Cunningham, B. T., Schaeffer, D. J., & Griffon, D. J. (2010). Cartilage tissue engineering on fibrous chitosan scaffolds produced by a replica molding technique. *Journal of Biomedical Materials Research - Part A*, *93*(1), 46–55. https://doi.org/10.1002/jbm.a.32514

Rajeswari, A., Sreerag Gopi, E., Christy, J. S., Jayaraj, K., & Pius, A. (2020). Current research on the blends of chitosan as new biomaterials. In T. Sabu, A. Pius, & S. Gopi (Eds.), *Handbook of Chitin and Chitosan* (1st ed., pp. 248–275). Elsevier Inc. https://doi.org/10.1016/B978-0-12-817970-3.00009-2

Raju, C. H. L., Rao, J. L., Reddy, B. C. V., & Brahmam, K. V. (2007). Thermal and IR studies on copper doped polyvinyl alcohol. *Bulletin of Materials Science*, *30*(3), 215–218. https://doi.org/10.1007/s12034-007-0038-1

Rinaudo, M. (2006). Chitin and chitosan: Properties and applications. *Progress in Polymer Science (Oxford)*, *31*(7), 603–632. https://doi.org/10.1016/j.progpolymsci.2006.06.001

Rojas-Martínez, L. E., Flores-Hernandez, C. G., López-Marín, L. M., Martinez-Hernandez, A. L., Thorat, S. B., Reyes Vasquez, C. D., Del Rio-Castillo, A. E., & Velasco-Santos, C. (2020). 3D printing of PLA composites scaffolds reinforced with keratin and chitosan: Effect of geometry and structure. *European Polymer Journal*, *141*(August), 1–10. https://doi.org/10.1016/j.eurpolymj.2020.110088

Shah, D. U. (2014). Natural fibre composites : Comprehensive Ashby-type materials. *Materials & Design*, *62*(May), 21–31.

Sikorski, D., Gzyra-Jagieła, K., & Draczyński, Z. (2021). The kinetics of chitosan degradation in organic acid solutions. *Marine Drugs*, *19*(5), 1–16. https://doi.org/10.3390/md19050236

Staroszczyk, H., Sztuka, K., Wolska, J., Wojtasz-Pająk, A., & Kołodziejska, I. (2014). Interactions of fish gelatin and chitosan in uncrosslinked and crosslinked with EDC films: FT-IR study. *Spectrochimica Acta - Part A: Molecular and Biomolecular Spectroscopy*, *117*, 707–712. https://doi.org/10.1016/j.saa.2013.09.044

Xie, W., Xu, P., Wang, W., & Liu, Q. (2002). Preparation of water-soluble chitosan derivatives and their antibacterial activity. *Journal of Applied Polymer Science*, *85*(7), 1357–1361. https://doi.org/10.1002/app.10424

Xu, P., Li, J., Meda, A., Osei-Yeboah, F., Peterson, M. L., Repka, M., & Zhan, X. (2020). Development of a quantitative method to evaluate the printability of filaments for fused deposition modeling 3D printing. *International Journal of Pharmaceutics*, *588*(May), 119760. https://doi.org/10.1016/j.ijpharm.2020.119760

Zhang, Z. Z., Zhang, H. Z., & Zhang, Z. Y. (2019). 3D printed poly(ε-caprolactone) scaffolds function with simvastatin-loaded poly(lactic-co-glycolic acid) microspheres to repair load-bearing segmental bone defects. *Experimental and Therapeutic Medicine*, *17*(1), 79–90. https://doi.org/10.3892/etm.2018.6947